PAPER

Calculation of Longitudinal Conversion Loss and Input Impedance for Indoor AC Mains Line Considering High-Speed PLC

A.K.M. Mahbub Ar RASHID[†], *Student Member*, Nobuo KUWABARA[†a)], Masahiro MAKI[††],
Yoshiharu AKIYAMA[†††], *and* Hiroshi YAMANE[†††], *Members*

SUMMARY The power line communication (PLC) system should be investigated with respect to the influence on electromagnetic environments. Longitudinal conversion loss (LCL) and input impedance are important parameters for evaluating the influence because they are closely related to the radiated, conducted, and inducted emission. An indoor AC mains system consisting of electrical equipment and an AC mains line was modeled by four-port networks, and the LCL and the input impedance were calculated. The parameters of the four-port networks were determined from theory and measurement. The analytical model was examined using a simple network and the results show that the calculated values agreed with the measured ones. The LCL and the input impedance were investigated at the AC mains port in some existing buildings, and the measured results almost agreed with the calculated results derived from the indoor AC mains system model.
key words: LCL, PLC, four-port F-matrix, common-mode impedance

1. Introduction

Recently, a power line communication (PLC) system that uses an AC mains line as the transmission line has been proposed. However, AC mains lines are not designed to act as telecommunications lines and many electric appliances are connected to them. Moreover, electromagnetic disturbances are emitted from AC mains lines due to radiation, conduction, and induction because of the poor performance at transmitting high frequency signals. Therefore, the influence of high-speed PLC signals on the electromagnetic environment has been studied [1], [2].

Longitudinal conversion loss (LCL) and input impedance are important parameters for evaluating the influence on the electromagnetic environment. These have already been evaluated for telecommunication lines [3], [4]. An emission reduction system has also been presented based on LCL values [2]. The investigation results for other mechanisms also suggest that conduction and induction are closely related to the LCL value [5]–[7]. However, the relationships between the configuration of the AC mains line and the LCL have not been clarified yet. A method for calculating the

LCL and the input impedance is needed to solve this problem.

In this paper, we described a method for calculating the LCL and the input impedance for an indoor AC mains system. The system is modeled based on the construction of a Japanese AC mains system and is represented by four-port networks. Using these networks, the LCL and the input impedance are calculated. To confirm the validity of the model, the calculated results are compared with measured results for a simple network. Finally, the calculated LCL and input impedance values obtained using the model were compared with measured values of those of an actual AC mains line.

2. Modeling of AC Mains Line

The configuration of the indoor AC mains system changes depending on the kind of appliances connected it, the size of the home, and the operating manner. Therefore, the AC mains line in an indoor environment should be modeled to calculate the LCL and the input impedance. The model of the indoor AC mains line used in this study is shown in Fig. 1. Statistics in Japan indicates that there are 3 to 6 branches from the panel board and branches have plug sockets and lights [8]. Thus, we assumed that there is one branch for about every $17\,m^2$. Moreover, a survey showed that the cable length of each branch is about $10\,m$ and even the longest branch is dozens of meters [8].

In this paper, we use a simple house model, about $40\,m^2$ in area, where one or two people live, because, in a complex model, it becomes difficult to explain the analyt-
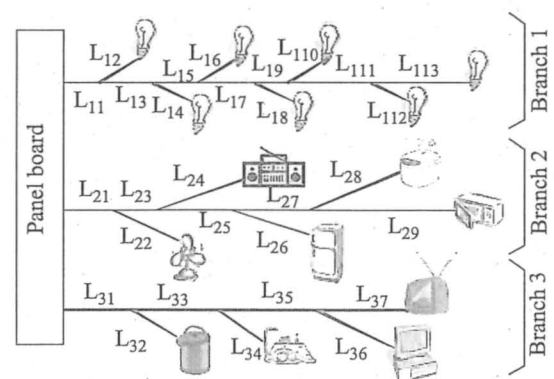

Fig. 1 Model of AC mains line.

Table 1 Cable lengths of the topology in meters ($i = 1, 2, 3$).

Line no.	Branch1	Branch2	Branch3
L_{i1}	0.5	1.0	1.5
L_{i2}	1.4	3.0	3.5
L_{i3}	0.25	0.5	2.0
L_{i4}	2.5	6.0	4.2
L_{i5}	0.25	1.5	0.5
L_{i6}	3.0	5.0	4.0
L_{i7}	0.75	1.0	4.5
L_{i8}	1.5	4.0	-
L_{i9}	0.25	5.0	-
L_{ia}	2.0	-	-
L_{ib}	1.1	-	-
L_{ic}	3.0	-	-
L_{id}	2.0	-	-

ical method and the amount of calculation for this type of house is not small. This contains three branches: one for lights, and the other two for plug sockets connected to home appliances. Each branch has at least three sub-branches and various electrical appliances are connected to the end of the sub-branches.
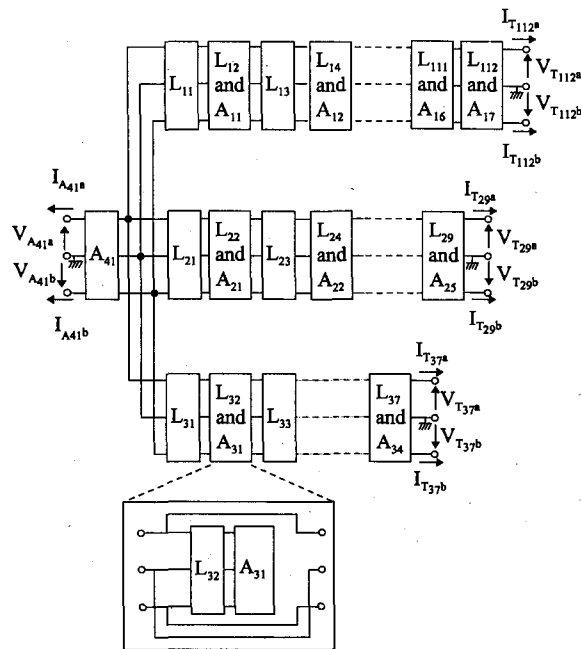
The lengths of cables for each branch and sub-branch are summarized in Table 1. The lengths were selected considering the actual power line wiring of an ordinary house [8]. We also assumed that at most ten electrical appliances of various kinds are connected to the power line at the same time.

In our study, we used VVF (PVC-insulated PVC-sheathed cable flat type) cable with two wires, which is widely used for indoor power lines in Japan.

3. Analysis Method

An AC mains line with a ground can be represented using four-port networks as shown in Fig. 2. In this figure, L_{nm} is an AC mains cable with a ground, A_{nm} is an appliance with ground, and A_{41} is the input impedance of a public AC mains line from the panel board. In this study, we used the artificial mains network (AMN) [9] as a model of the public AC mains line. In Japan, one wire of the AC mains cable is grounded at the transformer on a utility pole, so the public AC mains line is not a balanced line. AMN is designed based on foreign AC mains line and is a balanced network. However, the measurement results indicate that an AC mains line can be considered as a balanced line in the frequency range used by the high-speed PLC system though a suitable model has not yet been presented for AC mains lines in Japan. Therefore, we used AMN as a model of the public AC mains line. An appliance is connected to the bus line of the AC mains. Then, the appliance terminates the bus line via an AC mains cable as shown in Fig. 2. The parameters of four-port networks are determined from calculated values for an AC mains cable [3], [10] and measured values for appliances. The method of modeling the electrical appliance is described in the next subsection.

The input impedance and LCL are calculated from the relationships between the input voltage and current at a plug
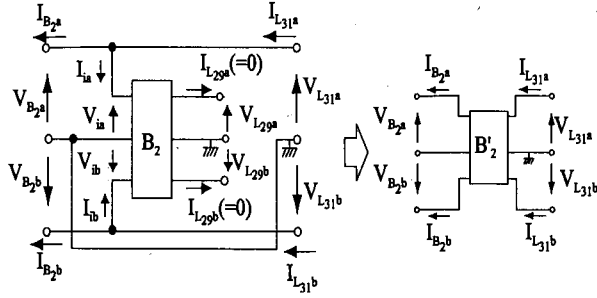

Fig. 2 Analysis method of LCL for AC mains line represented by four-port networks.

Fig. 3 Simplified model of AC mains line in Fig. 2 to calculate input impedance and LCL.

socket. Although the relationships can be obtained for any configuration of AC mains line, it is complex to explain the procedure for the universal case. Therefore, in this paper, we explain a calculation example that can easily be applied to other configurations.

In this paper, the input impedance and LCL are calculated at the plug socket connected to appliance A_{31} as an example. In this case, the analytical model in Fig. 2 is represented by the simple model shown in Fig. 3. Here, B_1, B_2, and B_{31} are matrices represented by the four-port networks in Fig. 2, and they are given by

$$[B_1] = [L_{11}][T_{12}][L_{13}][T_{14}][L_{15}]$$
$$\cdots\cdots[L_{110}][T_{111}][T_{112}] \qquad (1)$$
$$[B_2] = [L_{21}][T_{22}][L_{23}][T_{24}]$$
$$[L_{25}][T_{26}][L_{27}][T_{28}][T_{29}] \qquad (2)$$

Fig. 4   F-matrix model of the branch.

$$[B_{31}] = [L_{33}][T_{34}][L_{35}][T_{36}][T_{37}] \tag{3}$$

where L_{nm} are the four-port F-matrices representing the AC mains cable with ground, and $[T_{nm}]$ are the four-port F-matrices representing the load impedances of the line L_{nm} and the appliance A_{nm}. The method of calculating $[T_{nm}]$ is described in the appendix. In Fig. 3, I_{ina} and I_{inb} are the current sources representing the communication signal and the conductive disturbances of the appliance. Their actual values are not important in this paper because we consider only LCL and common mode input impedances here, so we set $I_{ina} = I_{inb} = 1$ to calculate LCL and $I_{ina} = -I_{inb} = 1$ to calculate input common-mode impedance.

The matrices $[B_1]$, $[B_2]$, and $[B_{31}]$ can be replaced by four-port matrices. The replacement procedure is summarized in Fig. 4, which shows the case of $[B_2]$ as an example. $[B_2]$ can be represented by the following equation.

$$\begin{bmatrix} [V_i] \\ [I_i] \end{bmatrix} = \begin{bmatrix} [A_{B_2}] & [B_{B_2}] \\ [C_{B_2}] & [D_{B_2}] \end{bmatrix} \begin{bmatrix} [V_{L_{29}}] \\ [I_{L_{29}}] \end{bmatrix} \tag{4}$$

The expressions of the matrices $[V_i]$, $[I_i]$, $[V_{L_{29}}]$, $[I_{L_{29}}]$, $[A_{B_2}]$, $[B_{B_2}]$, $[C_{B_2}]$, and $[D_{B_2}]$ are similar to the expressions in the appendix. From Fig. 4, we get

$$[I_{L_{29}}] = [0] \tag{5}$$

From Eq. (4), we get

$$[I_i] = [C_{B_2}][A_{B_2}]^{-1}[V_i] \tag{6}$$

From Fig. 4, the following relationships can be obtained

$$[V_{B_2}] = [V_{L_{31}}] = [V_i] \tag{7}$$

$$[I_{B_2}] = [I_i] + [I_{L_{31}}] \tag{8}$$

Then we get the F-matrix of $[B_2']$,

$$\begin{bmatrix} [V_{B_2}] \\ [I_{B_2}] \end{bmatrix} = \begin{bmatrix} [E] & [0] \\ [Y_{B_2}] & [E] \end{bmatrix} \begin{bmatrix} [V_{L_{31}}] \\ [I_{L_{31}}] \end{bmatrix} = [B_2'] \begin{bmatrix} [V_{L_{31}}] \\ [I_{L_{31}}] \end{bmatrix} \tag{9}$$

where $[E]$ is a unit matrix and $[0]$ is a zero matrix. From Eq. (6), $[Y_{B_2}]$ is given by

$$[Y_{B_2}] = [C_{B_2}][A_{B_2}]^{-1} \tag{10}$$

The matrices $[B_1]$ and $[B_{31}]$ can be replaced by $[B_1']$ and $[B_{31}']$ using the above procedure. Then, the model in Fig. 3 can be represented by the series connection of the four-port
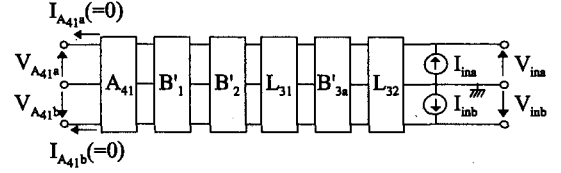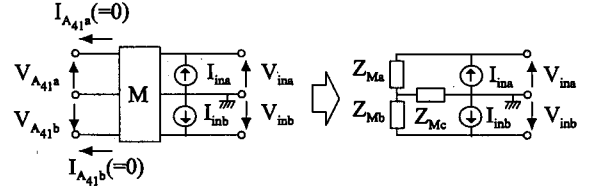

Fig. 5   Series connection of the four-port F-matrix.

Fig. 6   Equivalent circuit of input impedance at terminal of appliance A_{32}.

F-matrices shown in Fig. 5. From the model in Fig. 5, four-port F-matrix $[M]$ can be obtained as follows.

$$[M] = [A_{41}][B_1'][B_2'][L_{31}][B_{31}'][L_{32}] \tag{11}$$

Using a similar process to that from Eqs. (4) to (6), we get

$$[I_{in}] = [C_M][A_M]^{-1}[V_{in}] \tag{12}$$

Then,

$$[V_{in}] = [A_M][C_M]^{-1}[I_{in}] = [Z_M][I_{in}]$$
$$= \begin{bmatrix} Z_{M11} & Z_{M12} \\ Z_{M21} & Z_{M22} \end{bmatrix}[I_{in}] \tag{13}$$

The impedance matrix $[Z_M]$ can be expressed by a T-network as shown in Fig. 6. The parameters Z_{Ma}, Z_{Mb}, and Z_{Mc} are given by

$$Z_{Ma} = Z_{M11} - Z_{M12} \tag{14}$$

$$Z_{Mb} = Z_{M22} - Z_{M12} \tag{15}$$

$$Z_{Mc} = Z_{M12} \tag{16}$$

From the T-network parameters, we get LCL, differential-mode impedance Z_0, and common-mode impedance Z_L as follows [4], [11].

$$LCL(dB) = 20\log_{10}\left|\frac{-(Z_a - Z_b)^2 + 2Z_0(2Z_0 + 4Z_c)}{2Z_0(Z_a - Z_b)}\right| \tag{17}$$

$$Z_0 = Z_a + Z_b \tag{18}$$

$$Z_L = \frac{Z_a Z_b}{Z_a + Z_b} + Z_c \tag{19}$$

4.   Modeling Method of Household Appliances

A configuration of household appliances connected to an AC mains line is shown in Fig. 7. In this figure, Z_{A_i1}, Z_{A_i2}, and Z_{A_i3} are Δ-network parameters shown in Fig. 7, and the black rectangles represent the electrodes of an AC mains plug.
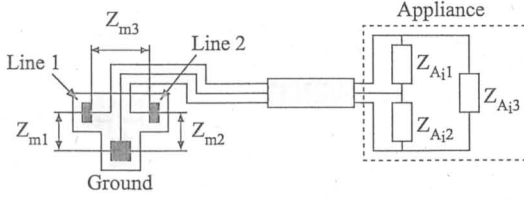
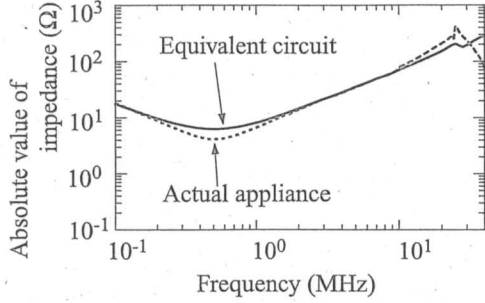**Fig. 7**   Measurement method of Δ-network parameters for appliances.

Fig. 8   Comparison between measured and modeled impedance of an appliance.

Fig. 9   Equivalent circuit for input impedance of a microwave oven.

The Δ-network parameters were obtained from measurements. We can measure input impedances Z_{m1}, Z_{m2}, and Z_{m3} of an appliance as shown in Fig. 7, where these impedances do not include the input impedance of AC mains lines because the power supply plug is not connected to the line. Therefore, AC mains power is not supplied to the appliance. The relationships between Z_{A_i1}, Z_{A_i2}, and Z_{A_i3} and Z_{m1}, Z_{m2}, and Z_{m3} are given by

$$Z_{A_i1} = \frac{Z_{m3}(1 + K)K_1}{K} \tag{20}$$

$$Z_{A_i2} = \frac{Z_{m3}(1 + K)K_3}{K} \tag{21}$$

$$Z_{A_i3} = \frac{Z_{m3}(1 + K)}{K} \tag{22}$$

where

$$K_1 = \frac{(Z_{m1} - Z_{m3})(Z_{m3} - Z_{m2}) + Z_{m1}Z_{m2}}{Z_{m2}Z_{m3} - Z_{m1}Z_{m3} + Z_{m3}^2} \tag{23}$$

$$K_2 = \frac{(Z_{m1} - Z_{m3})(Z_{m3} - Z_{m2}) + Z_{m1}Z_{m2}}{Z_{m2}Z_{m3} - Z_{m1}Z_{m2} + Z_{m2}^2} \tag{24}$$

$$K_3 = K_1 + K_3 \tag{25}$$

$$K = \frac{K_1}{K_2} \tag{26}$$

An example of the impedance characteristics of a microwave oven is shown in Fig. 8. The absolute value of the impedance Z_{A_i1} indicates that the input impedance of the appliance can be represented by an equivalent circuit because the frequency characteristics are simple. The equivalent circuit of the input impedance of a microwave oven is shown in Fig. 9. This circuit was modeled from the frequency characteristics of an actual microwave oven using a simulation tool, SPICE. The frequency characteristics of the equivalent circuit are also shown in Fig. 8. The characteristics of the
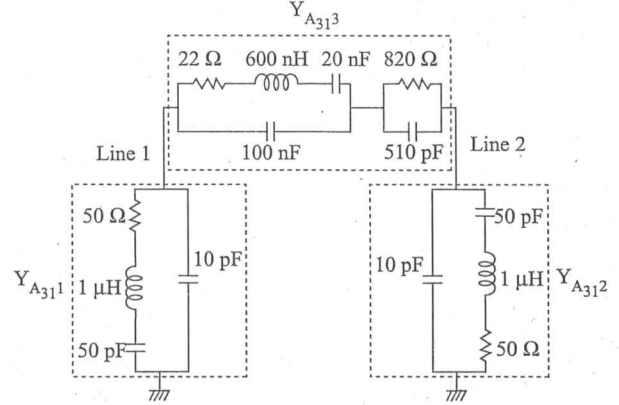
circuit almost agree with the measured ones up to 20 MHz. This means that we can use the equivalent circuit to evaluate the LCL and the input impedance.

Other appliances were also represented by equivalent circuits similar to the one shown in Fig. 9. They can express the frequency dependence although frequency characteristics of the equivalent circuit do not agree with those of the actual appliance at frequencies above 10 MHz.

It is important to study the relationships between the equivalent circuits and the actual circuits of appliances. This remains future work because of its difficulty.

5.   Experiment for the Validation of Analysis Method

To verify the analysis model shown in Fig. 2, we compared the calculated LCL and input impedance values with ones measured for a simple network.

5.1   Experimental Setup

For simplicity, we considered only branch 2 of the AC mains line model shown in Fig. 2. The experimental setup is shown in Fig. 10. An AC mains line was constructed on the conductive ground plane at a height of 5 cm. Appliances were represented by their equivalent circuits. The setup in Fig. 10 represented the case when AC mains power was not supplied to appliances because the equivalent circuits were determined when the power was not supplied. The method described in the previous section was used to determine the equivalent circuits of appliances.

The input impedances between two lines as well as of each line and ground were measured with an impedance analyzer. These impedances were converted into the impedances of a Δ-network (Z_{A_i1}, Z_{A_i2}, and Z_{A_i3}) by the same procedure as described in the previous section. They were converted again into the impedances of a T-network (Z_{Ma}, Z_{Mb}, and Z_{Mc}). Then LCL, differential-mode impedance, and common-mode impedance values were calculated using Eqs. (17) to (19).
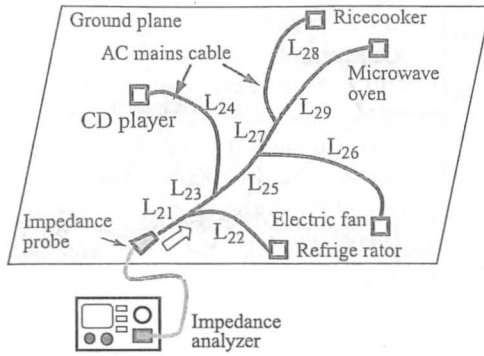
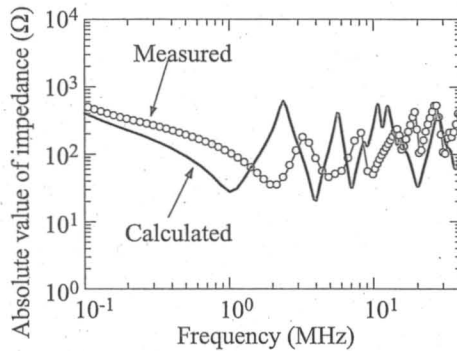**Fig. 10** Experimental setup for measuring LCL and input impedance.

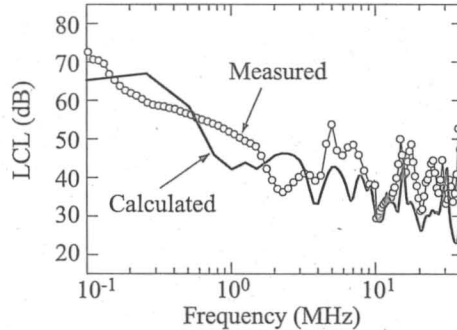**Fig. 11** Comparision between measured and calculated common-mode impedance characteristics.

Fig. 12 Comparision between measured and calculated LCL characteristics.

5.2 LCL Measurement Result

The results of measured and calculated impedance frequency characteristics are shown in Fig. 11. Here, we present only common-mode impedance Z_L. The solid line and circles indicate calculated and measured values, respectively. They indicate that the calculated values agree with the measured ones.

The LCL was obtained by using these input impedances. The measured and calculated LCL values are shown in Fig. 12. The solid line and circles represent the calculated and measured results respectively. The calculated LCL values almost agree with the measured ones.

These results indicate that the analysis method described in Sect. 3 and 4 can be used to estimate LCL and the input impedance of the analytical model shown in Fig. 2.

6. LCL for Actual AC Mains Line

The proposed analytical model was applied to an actual AC mains line and the calculated values were compared with the measured ones. This section describes the results.

6.1 Measurement of Input Impedance for Actual AC Mains Lines

We measured the input impedances of actual AC mains lines at several points in our laboratory building and in a house. The measurement points in the laboratory building are shown in Fig. 13. Four positions in the building were selected. The measurement room in Fig. 13 is the shielding room where the AC mains line is connected to a public AC line via a filter and isolation transformer. Other points are directly connected to a public AC line.

The experimental setup for measuring input impedance is shown in Fig. 14. A capacitor and transformer were inserted between the outlet and impedance probe to protect the probe from high AC voltage. We compensated for the influence of the transformer using the calibration function of the impedance analyzer but not for the influence of the capacitance, which was not significant because the absolute value of the impedance of the capacitance is less than $4\,\Omega$ from 0.1 MHz to 40 MHz and $1\,\Omega$ from 0.1 MHz to 10 MHz.

In the same way as described in Sect. 4, the input impedances Z_{m1}, Z_{m2}, and Z_{m3} were measured and the differential mode impedance and the common mode impedance were calculated from these measured data by the same procedure as described in the previous section.

The measured and calculated values for common-mode input impedance are shown in Fig. 15. Input impedances were measured at five points: the four points shown in Fig. 13 and another point in the AC mains port in a house. The average and standard deviation were calculated from those data. Although the common mode input impedance changed from $1\,\Omega$ to $10\,k\Omega$, the deviation reduced above 1 MHz, and the mean values were around $100\,\Omega$ in this frequency range. The solid line in this figure indicates calculated values. For the calculation, the model in Fig. 2 was used. The four-port F-matrices of line L_{nm} were obtained by calculation [10], and the equipment matrices A_{nm} were obtained from the measurements described in Sect. 4. The A_{41} was represented by an artificial mains network [9]. The F-matrix of the network was obtained from the requirements of the specifications [9] using procedures similar to those presented in Sect. 4. This figure shows that the calculated value almost agrees with the measured one above 1 MHz.

Although the configuration of the line used in the experiment is different from the model in Fig. 1, a similar result was obtained. This suggests that the calculation results derived from the model shown in Fig. 1, which includes a
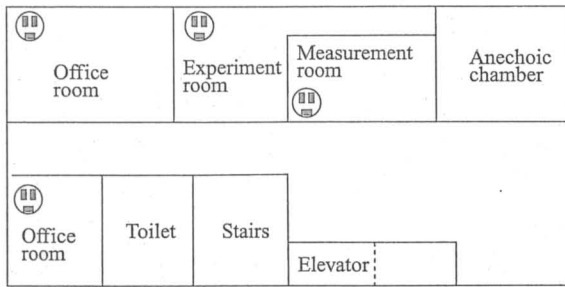
Fig. 13 Measurement points for input impedance of AC mains line (at laboratory building).
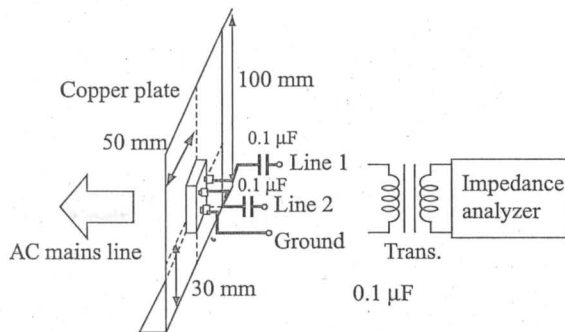

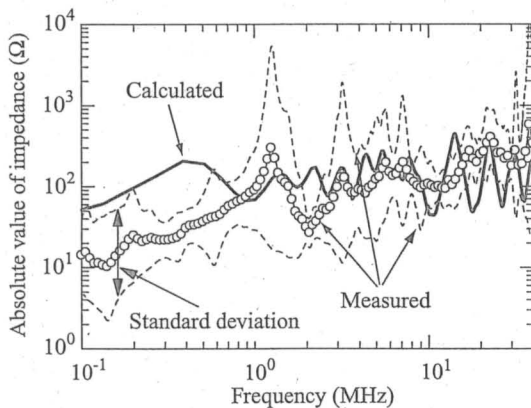Fig. 14 Measurement setup for input impedance of actual AC mains line.

Fig. 15 Measured and calculated common-mode impedance of actual AC mains line.

Fig. 16 LCL characteristics of actual AC mains line.

lot of equipment, cables, and a great deal of complexity, approach the typical calculation results. These results indicate that the model in Fig. 2 is effective for calculating the input impedance of an AC mains line.

6.2 Estimation of LCL for Actual AC Mains Line

The LCL of an actual AC mains line can be obtained from the measured input impedance by the process described in Sect. 6.1 and we calculated the average and standard deviation. The measured data was compared with the values calculated by the method described in Sect. 3. In the calculation, appliances in Fig. 2 were modeled from the measurement when the AC mains power was not supplied. Since
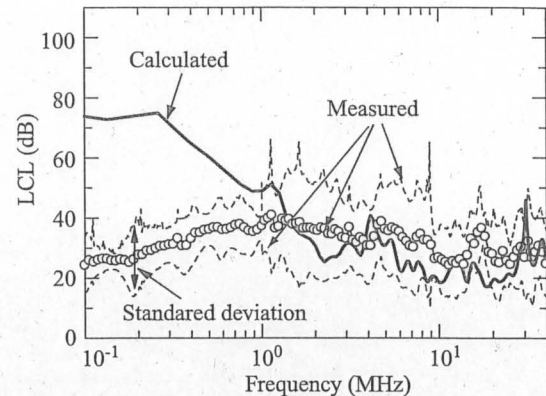
only one appliance was measured for each kind of appliances, the model used in the calculation did not represent these appliances.

They are shown in Fig. 16. In this figure, the solid line indicates the calculated values and the circles and dotted line indicate measured values for an actual AC mains line. The calculation results agree with the measured ones above 1 MHz as shown in this figure. This suggests that the model presented in this paper can only be used above 1 MHz because of the difference between the model and the AC mains line where one wire of the line is grounded at the transformer on a pole. This also suggests that the complexity of the model leads to the calculation results converging within the standard deviation of the measured values because the increase in the complexity converges the common-mode impedance and LCL within a certain range.

Since a high-speed PLC system is used in the frequency range of 2 MHz to 30 MHz [1], the model shown in Fig. 2 is effective for evaluating the influence on the electromagnetic environment because LCL and common mode impedance are important parameters for studying AC mains characteristics.

7. Conclusion

We investigated LCL and input impedance for indoor AC mains lines. An AC mains line in an indoor environment was modeled taking into consideration the wiring systems in typical small Japanese houses. In the analysis, the model was represented in a series connection of four-port F-matrices. The parameters of F-matrices were obtained from calculations of the line and measurements of appliances. The public mains line was represented by an artificial mains network. The LCL, differential mode impedance, and common mode impedance were calculated using this model.

An experiment using a simple network was carried out to confirm the validity of the model. The measurement values almost agreed with the calculated values.

The model was applied to calculate the LCL, differential mode impedance, and common mode impedance for an actual environment. The calculated values fell almost en-

tirely within the range of the standard deviation of the measurement results above 1 MHz although the configuration of the line used in the experiment was different from the model used in this paper. This suggests that the complexity of the model enables the calculation results to converge in the range of the standard deviation because the increase in complexity converges the common-mode impedance and LCL within a certain range. This means that the model presented in this paper is effective for evaluating the influence of the PLC system on electromagnetic environment in the frequency range of 2 MHz to 30 MHz.

A future work is to improve the calculation accuracy.

Acknowledgement

References

[1] Ministry of Public Management, Home Affairs, Posts and Telecommunications, "Announcement of report by power line communication study group," http://www.soumu.go.jp/jcho_tsusin/eng/index.html, Aug. 2002.

[2] Y. Khadour and H. Hirsch, "Reduction of the radiation in PLC system using a hybrid feeding," ICEMC 2002, pp.161–166, Bangkok, July 2002.

[3] Y. Shimoshio, M. Miyoshi, H. Koga, M. Tokuda, and T. Takai, "Characteristics of unbalance about earth and their calculation method for balanced cable with partial unbalance at arbitrary positions on it," IEICE Trans. Commun. (Japanese Edition), vol.J81-BII, no.9, pp.883–891, Sept. 1998.

[4] F. Amemiya, N. Kuwabara, and T. Ideguchi, "Method for estimating electromagnetic interference due to unbalance in telecommunication line," IEICE Trans. Commun., vol.E74-B, no.3, pp.141–147, March 1992.

[5] Y. Akiyama, H. Yamane, and N. Kuwabara, "Influence of a PLC signal induced into the modem on the communication performance of the VDSL," 2003 International Symposium on EMC, Istanbul, May 2003.

[6] Y. Shimoduma, A.K.M.M. Rashid, N. Kuwabara, Y. Akiyama, and H. Yamane, "A study of PLC signal influence on VDSL system by induction between power line and telecommunication line," EMC'04, pp.837–840, Sendai, June 2004.

[7] T. Tominaga, Y. Akiyama, H. Yamane, and N. Kuwabara, "Investigation of electromagnetic noise transmission characteristics from AC mains port to telecommunication port," IEEE EMC 2003, pp.505–510, Boston, MA, Aug. 2003.

[8] M. Maki, K. Tamesue, M. Tokuda, and N. Kuwabara, "The proposal of the power line transmission system using the MESA-code and the multi-band segmenting receiver," IEICE Trans. Fundamentals (Japanese Edition), vol.J65-A, no.6, pp.704–714, June 2002.

[9] IEC/CISPR Publication 22, third edition, "Information technology equipment—Radio disturbance characteristics—Limits and method of measurement," Nov. 1997.

[10] S. Hamada, T. Kawashima, J. Ochura, M. Maki, Y. Shimoshio, and M. Tokuda, "Influence of balance-unbalance conversion factor on radiated emission characteristics of balanced cables," IEEE EMC 2001, pp.31–36, Montreal, Canada, Aug. 2001.

[11] M. Hattori and T. Ideguchi, "Electromagnetic interference and coun-

termeasure on metallic lines for ISDN," ICC'89, pp.1214–1220, Boston, June 1989.

Appendix: Calculation Method of T_{nm}

As an example, we consider the case of L_{32} and A_{31} in Fig. 2, where L_{32} is the four-port F-matrix, and A_{31} is the 2-port impedance matrix as shown in Fig. A·1. Then, these matrices can be represented by

$$\begin{bmatrix} [V_i] \\ [I_i] \end{bmatrix} = \begin{bmatrix} [A_{L_{32}}] & [B_{L_{32}}] \\ [C_{L_{32}}] & [D_{L_{32}}] \end{bmatrix} \begin{bmatrix} [V_{L_{32}}] \\ [I_{L_{32}}] \end{bmatrix} \tag{A·1}$$

$$\begin{bmatrix} V_{L_{32}} \end{bmatrix} = \begin{bmatrix} Z_{A_{31}} \end{bmatrix} \begin{bmatrix} I_{L_{32}} \end{bmatrix} \tag{A·2}$$

where $[V_i]$ and $[I_i]$ are 1×2 matrices. They are represented as follows:

$$\begin{bmatrix} V_i \end{bmatrix} = \begin{bmatrix} V_{ia} \\ V_{ib} \end{bmatrix}, \quad \begin{bmatrix} I_i \end{bmatrix} = \begin{bmatrix} I_{ia} \\ I_{ib} \end{bmatrix} \tag{A·3}$$

A similar expression can be obtained in the case of $[V_{L32}]$ and $[I_{L32}]$.

$[A_{L_{32}}]$, $[B_{L_{32}}]$, $[C_{L_{32}}]$, and $[D_{L_{32}}]$ are 2×2 matrix. $[A_{L_{32}}]$ is represented as follows:

$$\begin{bmatrix} A_{L_{32}} \end{bmatrix} = \begin{bmatrix} A_{L_{32}11} & A_{L_{32}12} \\ A_{L_{32}21} & A_{L_{32}22} \end{bmatrix} \tag{A·4}$$

A similar expression can be obtained in the case of $[B_{L_{32}}]$, $[C_{L_{32}}]$, and $[D_{L_{32}}]$.

From Eqs. (A·1) and (A·2), we get

$$[V_i] = \begin{bmatrix} [A_{L_{32}}][Z_{A_{31}}] + [B_{L_{32}}] \end{bmatrix} [I_{L_{32}}] \tag{A·5}$$

$$\begin{bmatrix} I_i \end{bmatrix} = \begin{bmatrix} [C_{L_{32}}][Z_{A_{31}}] + [D_{L_{32}}] \end{bmatrix} [I_{L_{32}}] \tag{A·6}$$

From Fig. A·1, the following equations can be obtained.

$$[V_{L_{31}}] = [V_{T_{32}}] = [V_i] \tag{A·7}$$

$$[I_{L_{31}}] = [I_i] + [I_{T_{32}}] \tag{A·8}$$

Then we get the F-matrix of $[T_{32}]$,

$$\begin{bmatrix} [V_{L_{31}}] \\ [I_{L_{31}}] \end{bmatrix} = \begin{bmatrix} [E] & [0] \\ [Y_{T_{32}}] & [E] \end{bmatrix} \begin{bmatrix} [V_{T_{32}}] \\ [I_{T_{32}}] \end{bmatrix}$$

$$= \begin{bmatrix} T_{32} \end{bmatrix} \begin{bmatrix} [V_{T_{32}}] \\ [I_{T_{32}}] \end{bmatrix} \tag{A·9}$$
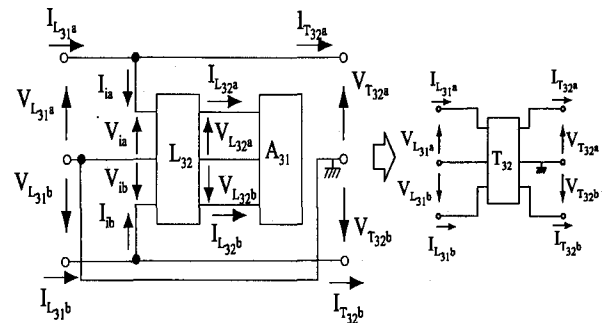

Fig. A·1   Analysis model of four-port F-matrix representing appliance with AC mains line.

where $[E]$ is a unit matrix, and $[0]$ is a zero matrix. From Eqs. (A·3) and (A·4), $[Y_{T_{32}}]$ can be represented by the following equation,

$$\left[Y_{T_{32}}\right] = \left[[C_{L_{32}}][Z_{A_{31}}] + [D_{L_{32}}]\right]$$
$$\cdot \left[[A_{L_{32}}][Z_{A_{31}}] + [B_{L_{32}}]\right]^{-1} \qquad \text{(A·10)}$$

Hiroshi Yamane received the B.E. and D.E. degrees from Ibaraki University in 1980 and 1997, respectively. After joining NTT, he has been researching lightning surge and overvoltage protection of telecommunication systems. He is the Manager of the Electromagnetic Environment Technology Group. He is a member of IEE. He recieved the Shibusawa Award in 2003 from Japan Electric Association.

A.K.M. Mahbub Ar Rashid was born in Dhaka, Bangladesh in 1978. He received the A.E. degree in electrical engineering from Kitakyushu National College of Technology and B.E. degree in electronic engineering from Kyushu Institute of Technology. Currently, he is a Master's student at the Graduate School of Electrical Engineering in the Kyushu Institute of Technology. His research areas are electromagnetic compatibility of communication systems, and power line communication.

Nobuo Kuwabara was born in Gifu, Japan in 1952. He received B.E. and M.E. degrees in electronic engineering from Shizuoka University in 1975 and 1977, respectively. He also holds a Dr. in Engineering from Shizuoka University, granted in 1992. Since joining NTT in 1977, he had been researching overvoltage protection of telecommunication systems, designing induction-free optical-fiber cables, and electromagnetic compatibility in telecommunication systems. At present, he is a professor in the faculty of engineering, Kyushu Institute of Technology. Dr. Kuwabara is a member of the IEEE and the IEE.

Masahiro Maki received the A.E. degree in electrical engineering from Oita National College of Technology in 1990, and B.E. and M.S. degrees in information engineering from Kyushu Institute of Technology in 1992 and 1994 respectively. He also holds a Ph.D. in Engineering from Kyushu Institute of Technology in 2002. Since joining Panasonic, he has been researching information communication system. Dr. Maki is a member of the IEEE

Yoshiharu Akiyama received the B.E. degree from the University of Electro Communications in 1990. After joining NTT, he has been researching EMC on wireless communications and home networking systems. He is a senior researcher in the EMC Technology Group.